nefrologia
Revista de la Sociedad Española de Nefrología
www.revistanefrologia.com

Original article

Unveiling the antiurolithiatic potentiality of two benzene sulfonamide derivatives against ethylene glycol-induced renal calculi

Ahmed M. Elgendy[a], Mohamed S. Nafie[b,c], Zohour I. Nabil[a], Nahla S. El-Shenawy[a,*], Heba N. Gad El-Hak[a]

[a] Zoology Department, Faculty of Science, Suez Canal University, Ismailia 41522, Egypt
[b] Department of Chemistry, College of Sciences, University of Sharjah, Sharjah 27272, United Arab Emirates (UAE)
[c] Chemistry Department, Faculty of Science, Suez Canal University, Ismailia 41522, Egypt

ABSTRACT

Objective: Oxidative stress and inflammation play crucial roles in the onset of kidney injury and crystal formation caused by hyperoxaluria. Indapamide is a potent medication for treating renal calculi, but it has severe side effects such as hypokalemia, hypercalcemia, and hyperuricemia. Therefore, it is advisable to explore alternative treatments that do not have these side effects. The study aimed to reveal the antiurolithiatic potential of two benzene sulfonamide derivatives (SBCl and SBF; A and B, respectively) against ethylene glycol-induced kidney stones.

Methods: The rats were divided into two main groups: the first group consisted of 20 rats with induced kidney stones, and the second group included 15 control rats. This division enabled a comparative analysis between rats with kidney stones and those without, offering insights into the effects of kidney stone induction on various physiological parameters and biochemical markers. The effectiveness of benzene sulfonamide derivatives (compounds A and B) was assessed in rats with induced kidney stones. The treatment was given orally by gavage for 21 days, administered every 48 h after inducing kidney stones with 0.12 ml of 5% ethylene glycol (EG).

Results: The influence of compounds A and B on electrolytes, biochemical, antioxidant, and inflammatory reactions in induced kidneys underscores their potential therapeutic advantages in alleviating the advancement of kidney stone disease and related complications.

Conclusion: Both compounds were found to possess equal effectiveness in inhibiting the complications of stone formation. However, SBCl-EG showed superior antioxidant and inflammatory parameters effects compared to SBF-EG. Our study's findings underscore the potential benefits of derivatives in treating nephrolithiasis and related oxidative disorders, highlighting their superior effects on antioxidant and inflammatory responses compared to standard treatments.

Divulgar la potencialidad antiurolitiásica de dos derivados de sulfonamida de benceno para combatir los cálculos renales inducidos por etilenglicol

R E S U M E N

Palabras clave:
Antioxidante
Inflamatorio
Hormonas
Histología
Microscopio electrónico
Rata

Objetivo: El estrés oxidativo y la inflamación juegan un papel esencial en la aparición de lesiones renales y la formación de cristales causadas por hiperoxaluria. Indapamida es una medicación potente para tratar los cálculos renales, pero tiene efectos secundarios graves tales como hipocalemia, hipercalcemia e hiperuricemia. Por tanto, es aconsejable explorar tratamientos alternativos que no tienen dichos efectos secundarios. El objetivo de este estudio fue revelar el potencial antiurolitiásico de dos derivados de sulfinamida de benceno (SBCl y SBF; A y B, respectivamente) para combatir los cálculos renales inducidos por etilenglicol.
Métodos: Se dividió a las ratas en dos grupos principales: el primero de ellos incluyó 20 ratas con cálculos renales inducidos, incluyendo el segundo 15 ratas de control. Dicha división permitió realizar un análisis comparativo entre las ratas con cálculos renales y las que carecían de ellos, proporcionando información sobre los efectos de la inducción de cálculos en diversos parámetros fisiológicos y marcadores bioquímicos. Se evaluó la efectividad de los derivados de sulfinamida de benceno (compuestos A y B) en ratas con cálculos renales inducidos. El tratamiento fue administrado oralmente mediante sonda durante 21 días, cada 48 h, tras la inducción de cálculos renales con 0,12 ml de 5% etilenglicol (EG).
Resultados: La influencia de los compuestos A y B en las reacciones electrolíticas, bioquímicas, antioxidantes e inflamatorias en los riñones inducidos destaca sus ventajas terapéuticas potenciales en cuanto a la mitigación del avance de los cálculos renales y sus complicaciones relacionadas.
Conclusión: Se encontró que ambos compuestos poseen igual efectividad a la hora de inhibir las complicaciones de la formación de cálculos. Sin embargo, SBCl-EG reflejó efectos superiores de los parámetros antioxidantes e inflamatorios en comparación con SBF-EG. Los hallazgos de nuestro estudio destacan los beneficios potenciales de los derivados a la hora de tratar la nefrolitiasis y los trastornos oxidativos relacionados, subrayando sus efectos superiores en las respuestas antioxidante e inflamatoria, en comparación con los tratamientos estándar.

Introduction

Animal models in kidney stone research provide valuable insights into the pathophysiology, prevention, and treatment of nephrolithiasis, or kidney stone formation.[1] These models, often developed in species such as rats, mice, or pigs, mimic various aspects of human kidney stone disease, allowing researchers to study the underlying mechanisms and test potential therapeutic interventions.[2]

Creating a kidney stone animal model generally involves inducing stone formation using various techniques, such as dietary manipulation, administering lithogenic substances, or performing surgical procedures.[3] For example, researchers may feed animals diets high in calcium, oxalate, or other stone-forming compounds to promote the formation of crystals within the kidneys. Alternatively, the development of calculi substances like ethylene glycol (EG) or ammonium oxalate may be administered to induce stone formation directly.[4] The EG serves as a metabolic precursor to oxalate, with oxalate formation typically initiated within 24–72 h

following its administration. This process can result in significant metabolic acidosis and acute kidney injury (AKI).[5]

After inducing kidney stones, researchers can observe the progression of stone formation, evaluate changes in renal function, and study related physiological responses. In addition, biochemical analyses of urine and blood samples provide valuable information on urinary stone risk factors, renal function markers, and systemic effects of stone formation.[6]

Renal calculi are a common urological issue marked by developing and sometimes expulsing crystal clusters within the urinary system. This condition, known as nephrolithiasis, originates from Greek roots: nephros (kidney), and lithos (stone).[7] Urolithiasis is prevalent worldwide, but its occurrence rate varies significantly due to gender, climate, diet, and other risk elements.[8]

There has been an annual rise in the incidence of stone formation among individuals aged 30 and above, irrespective of gender. Urolithiasis can manifest with diverse symptoms, including fever, vomiting, and loin pain, or it may even remain entirely asymptomatic.[9] Kidney stones are now acknowledged as a danger factor for various systemic illnesses such as

chronic kidney disease, diabetes, cardiovascular disease, and bone fractures. Conversely, these conditions also pose risk factors for developing kidney stones.[10] Renal function loss due to long-standing obstruction, and severe infections including septicemia.[11]

It is crucial to measure biochemical markers indicative of kidney function, such as serum levels of urea and creatinine, along with a panel of oxidative stress-related and inflammatory biomarkers.[12] Oxidative stress arises when there is an imbalance between oxidants and antioxidants, producing reactive oxygen species (ROS) that exceed the neutralizing ability of antioxidants.[13] This triggers a range of physiological and pathological reactions in cells and tissues. Also, the intricate interplay between factors like glycolipid metabolism abnormalities and hemodynamic changes activates processes such as the polyol and hexosamine pathways, leading to increased production of ROS.[14] ROS can act as second messengers in various signaling pathways and as regulators that influence the metabolism and apoptosis of immune cells.[15] Disrupting the oxidant/antioxidant balance in the kidneys initiates ROS, resulting in harmful outcomes like inflammation, autophagy, and fibrosis. These processes developed pathological and functional abnormalities in the kidneys.[16]

One factor contributing to kidney-related inflammation is acidosis, which increases intrarenal ammonia production.[17] This can partly activate the secretion of pro-inflammatory cytokines like IL-1β and IL-18. Substantial evidence shows that severe metabolic acidosis-induced increases in local ammonia concentration can stimulate maladaptive complement activation, resulting in heightened inflammatory and pro-fibrotic responses.[18]

Key inflammatory mediators causing kidney tissue damage include nitric oxide (NO) and ROS.[19] Consequently, it is believed that carbonic anhydrase inhibitors, such as benzene sulfonamide derivatives, might prevent the severe inflammation associated with this type of injury. ROS reacts with proteins and enzymes, causing lipid peroxidation (LPO) of cell and organelle membranes.[20] This reaction can lead to the breakdown of proteins, increased permeability of capillaries, and direct harm to the membranes of kidney cells. Additionally, NO causes renal injury by interacting with ROS and directly damaging renal tubules. It also diminishes the responsiveness of blood vessels to stagnant substances, worsening renal ischemia.[12]

Indapamide, classified as a thiazide-type diuretic, operates through a dual mechanism. It induces diuresis at the distal tubule in the kidney.[21] However, directly affects blood vessels, thus enhancing its effectiveness in lowering blood pressure. Indapamide shows promise in protecting organs affected by hypertension, such as the heart and kidneys.[22] Moreover, it boasts a favorable metabolic profile.[23] This array of benefits indicates that indapamide could serve as an effective and versatile treatment for hypertension, offering benefits beyond simply reducing blood pressure.[24] Indapamide has the potential to induce significant cases of both severe hypokalemia (low potassium levels) and hyponatremia (low sodium levels). Severe hyponatremia can cause the main clinical symptoms. During indapamide therapy, it is essential to monitor plasma sodium and potassium concentrations, particularly in patients who are at risk for hyponatremia and hypokalemia,

as is the case with other diuretics.[25] Explored alternative therapies devoid of these adverse effects and appropriate for the specific medical condition treated by Indapamide are advised.

Benzene sulfonamide derivatives, also known as sulfonamide derivatives, belong to a class of organic compounds that contain a sulfonamide functional group (–SO2NH2) attached to a benzene ring. These derivatives have applications in medicinal chemistry, agriculture, and industry for their versatile properties.[26] They have emerged as important therapeutic agents in other medical fields. For instance, certain sulfonamide drugs, such as acetazolamide and furosemide, are used as diuretics to treat conditions like edema and hypertension.[27] Additionally, sulfonamide-based drugs like celecoxib and indomethacin are widely prescribed as nonsteroidal anti-inflammatory drugs (NSAIDs) for their analgesic and anti-inflammatory properties in the management of pain and inflammation associated with conditions such as arthritis.[28] To the best of our knowledge, there is currently no available data regarding the effects of these new compounds on kidney stones.

So, the main target of the study was to measure the effect of benzene sulphonamide derivatives on kidney-induced stones in male albino rats by ethylene glycol and its possible protective role against kidney damage *in vivo*. The kidney damage assessment through the analysis of oxidative/antioxidant, inflammatory markers, hormonal levels, and histopathological responses could contribute to a better understanding of the mechanism of action and could be relevant for therapeutic purposes.

Materials and methods

Chemicals

The novel benzene sulfonamide derivatives combined with piperidine and morpholine,[29] represent a unique pharmacophore hybridization strategy. The compounds, exemplified by compound A (N-(4-chlorophenyl)-4-isobutoxy-N-(1-methylpiperidin-4-yl) benzene sulfonamide) and compound B (N-(4-fluorophenyl)-4-methoxy-N-(4-methylpiperidin-4-yl) benzene sulfonamide), was designed with a central scaffold of 4-alkoxy benzene sulfonamide. This scaffold incorporates three essential pharmacophore groups: piperidine, morpholine, and N-substituted piperazine moieties. The incorporation of these pharmacophores was carefully chosen due to their distinct structures and pharmacological advantages.

The presence of oxygen–nitrogen atoms in the morpholine structure and nitrogen–nitrogen atoms in the piperazine moiety enhances the pharmacological and pharmacokinetic profiles of the compounds. These atoms serve as hydrogen bond donors or acceptors, facilitating interactions with DNA and increasing water solubility and bioavailability. Furthermore, preserving the sulfonyl group within the compound's structure was favored over the carbonyl group because of its capacity to establish multiple hydrogen bonds with proteins. This feature backs the compounds' potential efficacy and specificity in biological systems.

Experimental animals and work design

About 35 male albino rats weighing 105 ± 10 g were maintained in plastic cages with stainless steel wire lids. They were housed for seven days for adaptation to laboratory conditions and fed *ad libithium*, before the initiation of the experiments under constant temperature and humidity. The rats were divided into two main categories; 1st group consisted of 20 rats with induced kidney stones and the 2nd one contained 15 rats serving as the control, comprised 15 rats. This division allowed for comparative analysis between rats with induced kidney stones and those without, providing insights into the effects of kidney stone induction on various physiological parameters or biochemical markers.

The effectiveness of benzene sulfonamide derivatives (compounds A and B) in induced kidney stone rats was evaluated. The treatment was administered orally via gavage for 21 days, with dosing intervals of every 48 h following the induction of kidney stones using 0.12 ml of 5% ethylene glycol. The handling and utilization of animals adhered strictly to the regulations and guidelines established by the Research Ethics Committee of the Faculty of Science, Suez Canal University, Ismailia, Egypt (number: REC166/2022). Furthermore, the experiment was conducted according to internationally accepted standard ethical guidelines for laboratory animal use and care, as outlined in the European Community guidelines.[30] The groups were divided as outlined below, with a sample size of 5 (Fig. 1). Treatment was administered to all groups every other day for 30 days.

1. The NEG group served as negative control animals.
2. The EG group (positive control) was treated with 0.12 ml of 5% ethylene glycol[31] for 21 days every 48 h to induce stone formation.
3. The SBCL-NEG group received treatment with 10 mg/kg of compound A without stone formation.
4. The SBCL-EG group was treated with 10 mg/kg of compound A after stone formation induced by ethylene glycol for 21 days.
5. The SBF-NEG group was treated with 10 mg/kg of compound B without stone formation.
6. The SBF-EG group received treatment with 10 mg/kg of compound B after stone formation induced by ethylene glycol for 21 days.
7. The IND-EG group was treated with 10 mg/kg of indapamide[31] after stone formation induced by ethylene glycol for 21 days.

Sample collection

After treatment, all rat groups were anesthetized with 50 mg/kg ketamine intraperitoneal.[32]

Blood sampling
Blood samples were obtained from the retro-orbital venous plexus using heparinized Hematocrit capillary tubes and promptly transferred into anticoagulant and clot activator tubes to facilitate serum separation.[33] The collected samples were left to stand at a slanting position for approximately 45 min at 4 °C. Following this, serum separation was achieved through centrifugation at 2500 rpm for 10 min. The acquired serum was stored at −20 °C and utilized for assessing the targeted kidney biomarkers and antioxidant, oxidative stress, and inflammatory markers.

Tissue collection
The kidney tissues were harvested and segmented into several portions to facilitate various analyses. Some tissue samples were frozen for biochemical analysis, while another set was fixed in 10% formalin for histopathological assessment. The remaining samples were kept in glutaraldehyde for examination using electron microscopy.

Electrolytes evaluation

Sodium (Na^+), potassium (K^+), ionized calcium (Ca^{2+}), and chloride ($Cl^−$) ions are measured using the ST-200 Plus electrolyte analyzer (Reagent pack: ST-200 Pro/Plus/CL) from SENSA CORE Company for Healthcare and Diagnostic Products.[34] These ions are directly measured by ion selective electrode (ISE). The magnesium (Mg^{2+}) test is conducted colorimetrically at wavelengths 520/800 nm, utilizing kits from the Beckman Coulter automated system. Inorganic phosphorus ($PO_4^−$) in serum is typically measured by forming a phosphomolybdate complex and then reducing it to a molybdenum blue color complex. The choice of reducing agents varies and includes stannous chloride, phenylhydrazine, amino naphthol sulfonic acid, ascorbic acid, p-methylamino phenol sulfate, N-phenyl-p-phenylenediamine, and ferrous sulfate.

Biochemical analysis in serum and tissues

All the parameters were determined using a Semi-automated chemistry analyzer BIOLAB ES-102 (Biomed diagnostics). The reagents were obtained from Diamond Diagnostics and Vitro Scient Kit, Cairo, Egypt.

Serum biomarkers of kidney
The determination of serum creatinine relies on the intensity of the color produced in the samples.[35] Serum urea undergoes enzymatic hydrolysis into ammonia (NH_4^+) and carbon dioxide (CO_2) within the sample. The resulting blood urea nitrogen reacts with salicylate and hypochlorite (NaClO), facilitated by the catalyst nitroprusside, to generate green indophenol at 578 nm and 37 °C.[36] Serum uric acid (UA) levels were determined by the method of Ref. 37.

Determination of oxalates in serum and urine
Oxalate oxidase catalyzes the oxidation of oxalate, producing hydrogen peroxide and carbon dioxide. In the presence of POD, hydrogen peroxide reacts with chromogenic substances, resulting in colored products. These products have a specific absorption peak at 550 nm, with the color intensity directly proportional to the oxalate concentration[38] (Karamad et al.[39]). The calculations were determined by plotting the standard curve using the OD values of the standards (*y*-axis) against their respective concentrations (*x*-axis) using the graphing software. The sample concentration is determined using the formula derived from the standard curve: $y = ax + b$. To calculate oxalate concentration: the curve is:
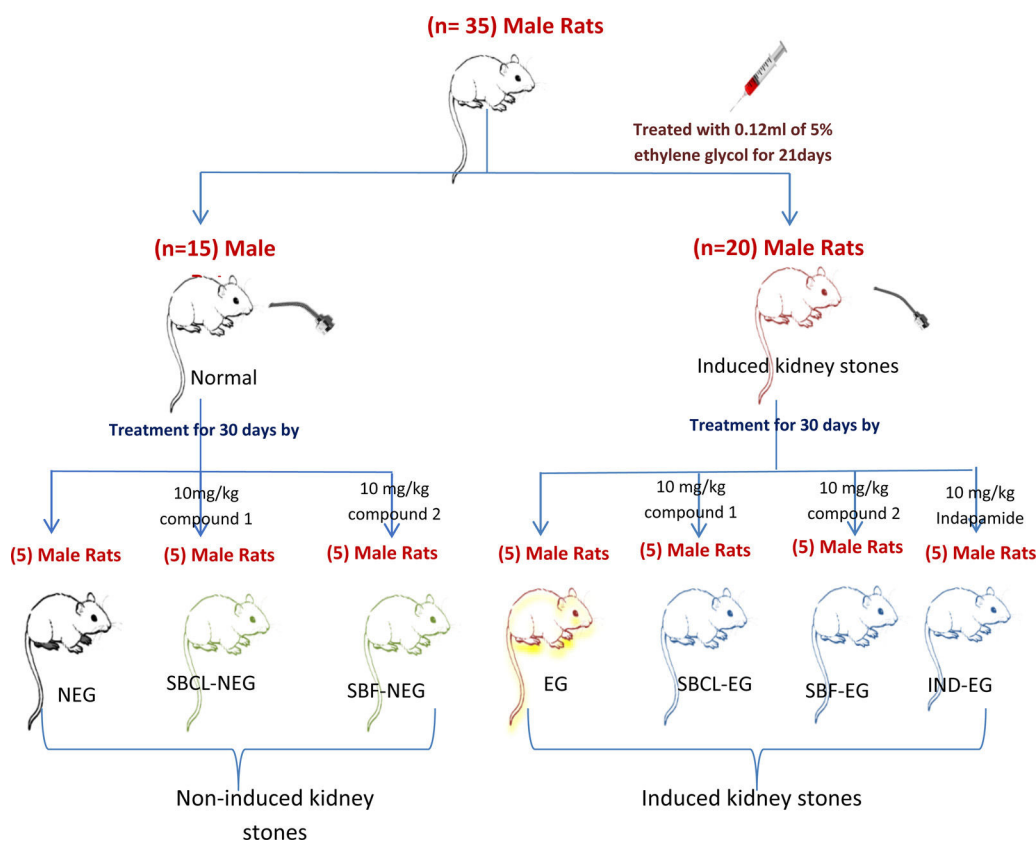
Fig. 1 – **The design of the experimental works.**

$y = ax + b$. The oxalate in urine $(mM/l) = (\Delta A - b)/a*2*f$ and the oxalate in serum $(mM/l) = (\Delta A - b)/a*f$ where ΔA is the change in absorbance, a and b are constants from the standard curve, and f is the dilution factor.

Determination of calcitonin and parathyroid
The ELISA kit employs the sandwich-ELISA method, utilizing a Microelisa strip plate pre-coated with an antibody specific to calcitonin (CT). The standards or samples in the appropriate wells interact with the specific antibody. Subsequently, a horseradish peroxidase (HRP)-conjugated antibody, specific for CT, is introduced to each well and allowed to incubate. TMB substrate solution is added to initiate color development, following washing to remove unbound components. Wells containing CT and HRP-conjugated CT antibodies exhibit a blue color, which turns yellow with the addition of the stop solution. The optical density (OD) at 450 nm was used to measure the concentration of CT spectrophotometrically.[39]

Parathyroid hormone (PTH) is measured using the fully automated Cobas e411 system. The test is completed within 18 min, involving the first and second incubation phases. The reaction mixture is aspirated into the measuring cell during the process, where the microplates magnetically adhere to the electrode surface. The application of voltage to the electrode triggers chemiluminescent emission, which is then quantified by a photomultiplier. Results are determined utilizing a calibration curve, which is instrument-specific and generated through a 2-point calibration process and a master curve.[40]

Determination of vitamin D3 (25 hydroxy cholecalciferol)
In this process, 25-hydroxy-vitamin D in the sample forms immune complexes with the monoclonal antibody present. At the same time, the antigenic determinant-DNA coupling template in reagent 2 binds to any remaining monoclonal antibodies. Unbound antigenic determinant-DNA coupling templates and dNTPs then undergo double-stranded DNA synthesis facilitated by polymerase. These products bind to fluorescent dyes, generating fluorescence proportional to the levels of 25-OH-VD in the samples.[40]

Renal tissue biomarkers of oxidative stress and antioxidant markers
10 mg tissue was homogenized on ice in 300 μl of the malondialdehyde (MDA) lysis buffer, then centrifuged to remove insoluble material. 200 μl of the supernatant from each homogenized sample was placed into a microcentrifuge tube. Assessing the end products of LPO is one of the most common assays for measuring oxidative damage. BioVision's LPO assay kit offers a convenient sensitive detection of MDA in samples.[41]

The tissue samples are homogenized in PBS (pH 7.4). It is essential to conduct these procedures at 4 °C. After centrifugation for 20 min at 2000–3000 rpm, the supernatant is carefully collected. Portions of the supernatant are aliquoted for ELISA assay and future experiments. The absorbance was measured at 450 nm using a microtiter plate reader.

The highly sensitive SOD assay kit employs WST-1, which produces a water-soluble formazan dye when reduced by the

superoxide anion. The reduction rate correlates directly with xanthine oxidase (XO) activity and is inhibited by SOD. Thus, SOD's inhibitory activity can be measured using a colorimetric method.[42]

Glutathione (GSH) is the primary intracellular low-molecular-weight thiol, crucial for defending mammalian cells against oxidative stress. BioVision's ApoGSHTM Glutathione Colorimetric Assay Kit offers a convenient and colorimetric approach for analyzing either total glutathione or specifically the reduced form of glutathione, utilizing a microtiter plate reader. This assay relies on the glutathione recycling system facilitated by DTNB and glutathione reductase.[43]

The ELISA kit employs the sandwich-ELISA method to evaluate the protein carbonyl (PC) level.[44]

Inflammatory markers in kidney tissues

The quantitative sandwich enzyme immunoassay technique was for interleukin-1β (IL-1β), interleukin-6 (IL-6), and alpha tumor necrosis factor (TNF-α) determination according to Çetin et al.[45]

Histopathology evaluation

The kidneys of each animal were rapidly removed and rinsed with normal saline (0.9% NaCl, Nile Pharm Company, Egypt) to eliminate any blood that might hinder the fixation process. They were then blotted with filter paper, weighed, rinsed in ice-cold saline, and fixed in 10% neutral formaldehyde (Sigma Aldrich Chemical Company, USA) overnight. Subsequently, the kidneys were processed using standard histological methods.[46] Blind pathologists evaluate the histopathological alteration.

Electron microscope examination of kidney tissues

Small kidney samples were excised and cut under a dissecting microscope in the presence of 2% glutaraldehyde. They were then fixed in 2% glutaraldehyde in 0.1 M Na-cacodylate buffer for 24 h, washed in 0.1 M phosphate buffer at 4 °C, and post-fixed in 1% osmium tetroxide. After being dehydrated in a graded series of ethyl alcohol, the tissues were infiltrated with resin. Semi-thin slices were prepared using an ultramicrotome, stained with toluidine blue, and examined under a light microscope. Selected fields of these sections were further sectioned into ultrathin slices, stained with uranyl acetate and lead citrate, and examined using a transmission electron microscope (JEOL JEM-2100, Japan) in the Electron Microscope Unit, Mansoura University.[47]

Statistical analysis

All data were presented as mean ± standard error (SE), with a significance level at $P < 0.05$ using SPSS 11.0 for Windows. Statistical differences were assessed using one-way analysis of variance (ANOVA), followed by post-hoc Duncan analysis.

Results

The effect of benzene sulfonamide was investigated by administration of benzene derivative compounds A (SBCL) and B (SBF) to male albino rats with induced kidney stones. The rats were divided into seven groups, each comprising five animals, and orally administered the benzene sulfonamide derivatives for four weeks following a three-week stone induction period. Samples were collected to assess kidney functions, antioxidant, anti-inflammatory, hormonal, and histopathology as outlined below.

Electrolytes

Table 2 illustrates the impact of SBCL and SBF on the blood ions of rats, including Na^+, K^+, Cl^-, Mg^{2+}, PO_4^-, and Ca^{2+}. Serum levels of Na^+, Cl^-, and Ca^{2+} exhibited no notable variance before and after stone induction following treatment with SBCL and SBF. Conversely, there was a significant reduction in K^+ levels after SBF treatment in rats with induced kidney stones, as compared to indapamide treatment, resulting in a 16% decrease in K^+ levels, as detailed in Table 1.

In rats with induced kidney stones, the administration of indapamide led to a notable decrease in Mg^{2+} levels by 29%, as indicated in Table 1. Specifically, Mg^{2+} levels declined from 1.36 ± 0.07 in the EG group to 0.96 ± 0.05 in the IND group. In comparison, the research revealed that SBCL treatments following stone induction led to Mg^{2+} levels that were 1.4 times higher compared to the group treated with indapamide, a conventional medication (Table 1).

The administration of SBCL and SBF to rats resulted in a statistically significant increase in the PO_4^{3-} level by 21% and 25% respectively (Table 1).

Renal biomarkers

The effects of compound A (SBCL) and compound B (SBF) on rat kidney functions, including creatinine, urea, blood urea nitrogen (BUN), and uric acid, are summarized in Table 2. Treatment of normal rats with SBCL and SBF resulted in a significant decrease in serum creatinine levels ($P \le 0.05$) compared to control animals. Induction of kidney stones in male albino rats leads to elevation of creatinine levels ($P \le 0.05$). Treatment of kidney stone rats with SBF or indapamide decreased the creatinine level significantly.

When normal rats were treated with SBCL and SBF, there was a significant decrease in blood urea and BUN levels. Conversely, treatment of induced kidney stone rats with indapamide standard medication caused a significant increase in urea and BUN levels. Additionally, SBF treatment significantly decreased urea and BUN levels compared to SBCL in induced kidney stone rats (Table 2).

Rats treated with SBF showed a marked increase in serum uric acid levels, rising from 1.40 ± 0.04 in the NEG group to 1.71 ± 0.03 mg/dl in the SBF-NEG group. Following stone induction, treatment with SBF or indapamide standard medication significantly decreased serum uric acid levels (Table 2). Furthermore, SBF exhibited a more significant decrease in serum uric acid as compared to SBCL in induced kidney stone rats.

Table 1 – Effect of compound A (SBCL) and compound B (SBF) treatment on serum electrolytes of induced kidney stones rats.

Parameters	NEG	SBCL-NEG	SBF-NEG	EG group	IND-EG	SBCL-EG	SBF-EG
Sodium (Na^+) (mmol/l)	144.63 ± 0.63	145.20 ± 0.46	143.64 ± 0.61	144.52 ± 0.67	144.94 ± 0.31	144.36 ± 0.46	144.22 ± 0.26
Potassium (K^+) (mmol/l)	6.01 ± 0.16	6.54 ± 0.15	5.79 ± 0.15	6.78 ± 0.04[a]	6.35 ± 0.10	5.85 ± 0.11	5.31 ± 0.14[d]
Ionized calcium (Ca^{2+}) (mmol/l)	1.32 ± 0.02	1.32 ± 0.01	1.26 ± 0.03	1.38 ± 0.02	1.30 ± 0.02	1.32 ± 0.01	1.29 ± 0.02[c]
Chloride (CL^-) (mmol/l)	97.83 ± 0.56	99.58 ± 0.49	99.50 ± 0.40	99.86 ± 0.27	100.70 ± 0.52	100.56 ± 0.44	98.20 ± 0.58
Magnesium (Mg^{2+}) (mg/dl)	1.20 ± 0.15	1.36 ± 0.07	1.44 ± 0.13	1.50 ± 0.07[b]	1.30 ± 0.06[b]	1.06 ± 0.05[b,d]	0.96 ± 0.13[b,c,d]
Phosphorous (PO_4^-) (mg/dl)	4.75 ± 0.13	6.00 ± 0.20[a]	5.06 ± 0.20	6.32 ± 0.21[a]	5.04 ± 0.12	5.24 ± 0.09	5.04 ± 0.09

Data were expressed as means ± SEM, $n = 5$. Data were statically analyzed using one-way ANOVA followed by Duncan multiple comparisons test $P \leq 0.05$. NEG, control negative; EG, control positive; SBCL-NEG, non-induced kidney stone group was treated with compound A; SBF-NEG, non-induced kidney stone group was treated with compound B; SBCL-EG, induced kidney stone group was treated with compound A; SBF-EG, induced kidney stone group was treated with compound B; IND-EG, induced kidney stone group was treated with indapamide. [a] referred to the comparison of SBCL-NEG, SBF-NEG, or EG with NEG was statistically significant. [b] referred to the comparison of IND-EG, SBCL-EG, or SBF-EG with EG was statistically significant. [c] referred to the comparison of SBCL-EG with SBF-EG as statistically significant. [d] referred to the comparison of SBCL-EG or SBF-EG with IND-EG was statistically significant. Sodium (Na^+) (mmol/l), potassium (K^+) (mmol/l), ionized calcium (Ca^{2+}) (mmol/l), chloride (CL^-) (mmol/l), magnesium (Mg^{2+}) (mg/dl), and phosphorous (PO_4^-) (mg/dl).

Table 2 – Effect of compound A (SBCL) and compound B (SBF) treatment on renal functions of induced kidney stones rats.

mg/dl	NEG	SBCL-NEG	SBF-NEG	EG group	IND-EG	SBCL-EG	SBF-EG
Creatinin (mg/dl)	0.77 ± 0.02	0.66 ± 0.02[a]	0.67 ± 0.02[a]	0.85 ± 0.03[a]	0.70 ± 0.02[b]	0.77 ± 0.02	0.67 ± 0.01[b,c]
Urea (mg/dl)	27.25 ± 0.85	24.0 ± 063[a]	26.4 ± 0.46	33.4 ± 0.96[a]	22.2 ± 1.43[b]	30.4 ± 0.46[d]	26.4 ± 0.91[c,d]
BUN (mg/dl)	13.73 ± 0.29	12.28 ± 0.31	12.34 ± 0.38	15.56 ± 0.44[a]	10.36 ± 0.67[b]	14.5 ± 0.38[d]	12.34 ± 0.42[c,d]
Uric acid (mg/dl)	1.40 ± 0.04	1.53 ± 0.11	1.71 ± 0.03[a]	1.41 ± 0.01	1.25 ± 0.06[b]	1.47 ± 0.03[d]	1.17 ± 0.05[c,d]

Data were expressed as means ± SEM, $n = 5$. Data were statically analyzed using one-way ANOVA followed by Duncan multiple comparisons test $P \leq 0.05$. NEG, control negative; EG, control positive; SBCL-NEG, non-induced kidney stone group was treated with compound A; SBF-NEG, non-induced kidney stone group was treated with compound B; SBCL-EG, induced kidney stone group was treated with compound A; SBF-EG, induced kidney stone group was treated with compound B; IND-EG, induced kidney stone group was treated with indapamide. [a] referred to the comparison of SBCL-NEG, SBF-NEG, or EG with NEG was statistically significant. [b] referred to the comparison of IND-EG, SBCL-EG, or SBF-EG with EG was statistically significant. [c] referred to the comparison of SBCL-EG with SBF-EG as statistically significant. [d] referred to the comparison of SBCL-EG or SBF-EG with IND-EG was statistically significant.

Determination of oxalates in serum and urine

Treating non-induced kidney stones in rats with SBCL and SBF showed a significant reduction in serum oxalate levels by a 2.5-fold decrease in SBCL compared to the negative control. Similarly, treating induced kidney stone rats with SBCL, SBF, or indapamide led to decreased oxalate levels (Fig. 2a).

The effect of SBCL and SBF on urine oxalates is illustrated in Fig. 2b. Kidney stone induction in rats resulted in a two-fold increase in urine oxalates compared to the negative control. Treatment of these rats with indapamide significantly reduced urine oxalates by 41% compared to the control. Similarly, treatment with SBCL significantly decreased urine oxalates by 32% compared to the control. Treatment with SBF also significantly reduced urine oxalate concentrations by 22.7%.

Parathyroid, calcitonin, and vitamin D3

The effect of SBCL and SBF treatment on PTH, calcitonin, vitamin D3, and citrate was demonstrated in Table 3. In non-induced kidney stone rats, the administration of SBF resulted in a noteworthy rise in PTH levels compared to SBCl. Specif-

ically, the induction of renal stones led to a statistically significant increase in PTH levels. In the SBF-EG group, the level of PTH declined more than indepamined and SBCl-EG-treated rats as compared to EG animals.

In induced kidney stone rats, both SBCL and indapamide treatments resulted in a significant increase in PTH levels. PTH levels notably rose from the EG-group baseline of 3.52 ± 0.56 to higher levels in SBCL-EG (5.16 ± 0.65) and IND-EG rats (5.2 ± 0.48). Conversely, the treatment involving SBF resulted in a statistical decrease in PTH levels compared to the EG group. The PTH levels decreased significantly from the baseline (4.52 ± 0.42) to a lower level in SBF-treated (SBF-EG) rats (3.42 ± 0.17). Interestingly, the treatment with SBF showed a statistical reduction in PTH levels compared to the SBCL-treated group ($P \leq 0.05$) (Table 3).

In kidney stones, induction by EG resulted in a notable statistical increase in serum calcitonin levels. Following stone induction, treatment with SBCL, SBF, and indapamide medication in rats exhibited a significant decrease in serum calcitonin levels. Specifically, SBCL treatment in induced kidney stone rats showed a more pronounced decline in calcitonin levels compared to SBF treatment. However, the treatment involving
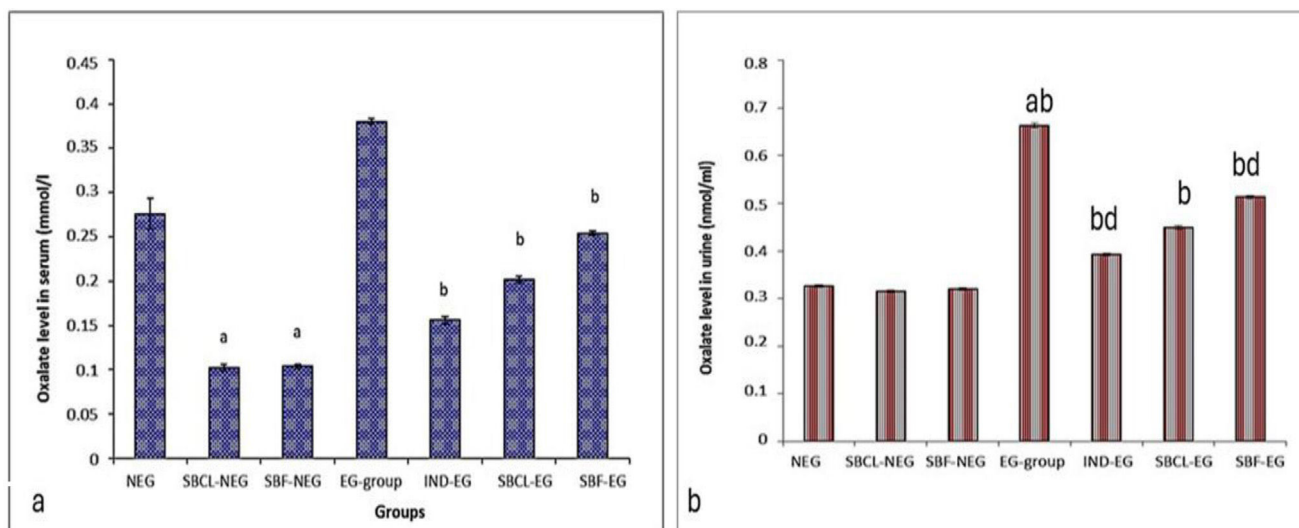
Fig. 2 – (a) Effect of compound A (SBCL) and compound B (SBF) treatment on serum oxalate levels. Data were expressed as means ± SEM, n = 5. Data were statically analyzed using one-way ANOVA followed by Duncan multiple comparisons test P ≤ 0.05. [a] referred to the comparison of SBCL-NEG, SBF-NEG, or EG with NEG was statistically significant. [b] referred to the comparison of IND-EG, SBCL-EG, or SBF-EG with EG was statistically significant. (b) Effect of compound A (SBCL) and compound B (SBF) treatment on urine oxalates. Data were expressed as means ± SEM, n = 6. Data were statically analyzed using one-way ANOVA followed by Duncan multiple comparisons test P ≤ 0.05. [a] letter referred to the comparison of SBCL-NEG, SBF-NEG, or EG with NEG was statistically significant. [b] letter referred to comparison of IND-EG, SBCL-EG, or SBF-EG with EG was statistically significant. [d] letter referred to the comparison of SBCL-EG or SBF-EG with IND-EG was statistically significant.

Table 3 – Effect of compound A (SBCL) and compound B (SBF) treatment on hormones, and vitamin D3 of induced kidney stones rats.

	NEG	SBCL-NEG	SBF-NEG	EG group	IND-EG	SBCL-EG	SBF-EG
Parathyroid hormone (PTH, pg/ml)	1.50 ± 0.30	1.98 ± 0.15	2.42 ± 0.16[a]	4.52 ± 0.42[a]	5.6 ± 0.32[b]	4.56 ± 0.40	3.28 ± 0.17[b,c,d]
Calcitonin (pg/ml)	42.83 ± 0.52	41.10 ± 0.34	41.17 ± 0.15	110.34 ± 0.78[a]	55.34 ± 0.23[b]	75.16 ± 0.42[b,c]	83.67 ± 0.43[b,c,d]
25 hydroxyl vitamin D (25OH-D3) (ng/ml)	14.04 ± 0.27	11.68 ± 0.22[a]	18.00 ± 0.12[a]	11.42 ± 0.26[a]	10.17 ± 0.12	18.64 ± 0.21[b,c]	17.44 ± 0.19[b]

Data were expressed as means ± SEM, n = 5. Data were statically analyzed using one-way ANOVA followed by Duncan multiple comparisons test P ≤ 0.05. NEG, control negative; EG, control positive; SBCL-NEG, non-induced kidney stone group was treated with compound A; SBF-NEG, non-induced kidney stone group was treated with compound B; SBCL-EG, induced kidney stone group was treated with compound A; SBF-EG, induced kidney stone group was treated with compound B; IND-EG, induced kidney stone group was treated with indapamide. [a] referred to the comparison of SBCL-NEG, SBF-NEG, or EG with NEG was statistically significant. [b] referred to the comparison of IND-EG, SBCL-EG, or SBF-EG with EG was statistically significant. [c] referred to the comparison of SBCL-EG with SBF-EG as statistically significant. [d] referred to the comparison of SBCL-EG or SBF-EG with IND-EG was statistically significant.

indapamide, a standard medication, resulted in a statistically more significant reduction in serum calcitonin levels as compared to SBCL and SBF treatments (Table 3).

In the comparison of SBCL and SBF treatment on serum 25hydroxy vitamin D (25OH-D3) in male albino rats, distinct effects were observed (Table 3). Treating non-induced kidney stone rats with SBCL resulted in a statistically significant decrease in 25OH-D3 levels. Conversely, SBF treatment demonstrated a significant increase, with levels decreasing from the baseline in the NEG group (14.04 ± 0.27) to SBCL-NEG rats (11.68 ± 0.22) and increasing to 18.00 ± 0.12 in SBF-NEG rats.

Inducing kidney stones led to a significant decrease in 25OH-D3 levels, reducing from the initial NEG levels (14.04 ± 0.27) to levels in the induced stone group (11.42 ± 0.26). Treating induced kidney stone rats with SBCL and SBF resulted in a significant increase in 25OH-D3 levels. In contrast, treatment with indapamide resulted in a statistically significant reduction in 25OH-D3 levels (Table 3).

Renal tissue oxidative/antioxidants

The impact of SBCL and SBF on tissue levels of GSH, NO, LPO, and PC as well as the activity of SOD is presented in Table 4.

	EG group	SBCL-EG	SBF-EG	EG group	IND-EG	SBCL-EG	SBF-EG
Table 4 – Effect of compound A (SBCL) and compound B (SBF) on antioxidants/oxidative stress and inflammatory biomarkers of induced kidney stones rats.							
LPO (nmol/mg)	0.14 ± 0.01	0.14 ± 0.01	0.14 ± 0.01	0.53 ± 0.01^a	0.23 ± 0.01^b	0.34 ± 0.01^b	$0.38 \pm 0.01^{b,c}$
NO (μmol/g)	5.32 ± 0.01	5.33 ± 0.01	5.34 ± 0.01	11.39 ± 0.08^a	6.93 ± 0.02^b	$8.58 \pm 0.02^{b,c}$	$9.65 \pm 0.06^{b,c}$
SOD (U/mg)	1.82 ± 0.05	1.84 ± 0.03	1.82 ± 0.02	0.51 ± 0.01^a	1.38 ± 0.01^b	1.17 ± 0.01^b	$0.99 \pm 0.02^{b,c}$
GSH (ng/mg)	6.85 ± 0.18	6.87 ± 0.03	6.85 ± 0.03	4.02 ± 0.05^a	6.06 ± 0.07^b	5.63 ± 0.05^b	5.04 ± 0.05^b
PC (ng/mg)	16.04 ± 0.17	15.98 ± 0.06	15.97 ± 0.03	31.13 ± 0.30^a	20.13 ± 0.17^b	22.18 ± 0.14^b	$24.35 \pm 0.21^{b,c}$
Interleukin-1β (pg/ml)	850.30 ± 10.56	846.98 ± 4.99	851.14 ± 4.41	$2171.27 \pm 20.7^{a,b}$	1069.8 ± 17.89^b	$1462.98 \pm 10.48^{b,c}$	$1646.08 \pm 12.05^{b,c,d}$
Interleukin-6 (pg/ml)	7.94 ± 0.16	7.83 ± 0.04	7.99 ± 0.05	18.50 ± 0.08^a	9.67 ± 0.07^b	11.95 ± 0.10^b	$13.26 \pm 0.10^{b,c}$
TNF-α (pg/ml)	34.79 ± 0.71	34.41 ± 0.37	35.05 ± 0.22	80.92 ± 0.85^a	42.10 ± 0.60^b	$56.90 \pm 0.56^{b,c}$	$62.34 \pm 0.57^{b,c,d}$

Data were expressed as means ± SEM, $n = 5$. Data were statically analyzed using one-Way ANOVA followed by Duncan multiple comparisons test $P \leq 0.05$. NEG, control negative; EG, control positive; SBCL-NEG, non-induced kidney stone group was treated with compound A; SBF-NEG, non-induced kidney stone group was treated with compound B; SBCL-EG, induced kidney stone group was treated with compound A; SBF-EG, induced kidney stone group was treated with compound B; IND-EG, induced kidney stone group was treated with indapamide. [a] referred to the comparison of SBCL-NEG, SBF-NEG, or EG with NEG was statistically significant. [b] referred to the comparison of IND-EG, SBCL-EG, or SBF-EG with EG was statistically significant. [c] referred to the comparison of SBCL-EG with SBF-EG as statistically significant. [d] referred to the comparison of SBCL-EG or SBF-EG with IND-EG was statistically significant. Glutathione (GSH), superoxide dismutase (SOD), nitric oxide (NO), lipid peroxidation (LP), protein carbonyl (PC), and tumor necrosis factor-alpha (TNF-α).

Induction of kidney stones in rats resulted in a statistically significant decrease in tissue GSH levels and SOD activity by 41.3% and 72%, respectively, compared to controls. However, treatment of induced kidney stones in rats with indapamide increased GSH and SOD by 1.5-fold and 2.7-fold, respectively, compared to controls. Additionally, treatment with SBCL increased GSH and SOD by 1.4-fold and 2.3-fold, respectively, compared to controls. Treatment of induced kidney stone rats with SBF showed a significant increase in tissue GSH and SOD by 1.3-fold and 1.9-fold, respectively, compared to controls (Table 4).

Induction of kidney stones in male albino rats resulted in a statistically significant increase in tissue NO by 2.1-fold, LPO by 3.8-fold, and PC by 1.9-fold compared to controls (Table 4). Treatment of induced kidney stone rats with indapamide resulted in a statistically significant decrease in tissue NO by 39%, LPO by 57%, and PC by 35% compared to controls.

Furthermore, treatment of induced kidney stone rats with SBCL led to a statistically significant decrease in tissue NO and LPO by 25% and 36%, respectively, as well as a 29% decrease in tissue PC compared to controls. Similarly, treatment with SBF resulted in a statistically significant decline in tissue NO and LPO by 15% and 28%, respectively, as well as a 22% decrease in tissue PC compared to controls ($P \leq 0.05$) (Table 4).

Renal tissue inflammatory biomarkers

The effect of treatment with compounds A (SBCL) and B (SBF) on tissue levels of IL-1β, IL-6, and TNF-α is presented in Table 4. Induction of kidney stones in rats led to a statistically significant increase in tissue IL-1β by nearly 2.6-fold, IL-6 by 2.3-fold, and TNF-α by 2.3-fold compared to controls ($P \leq 0.05$). Treatment of induced kidney stones in rats with indapamide resulted in a statistically significant decline in IL-1β, IL-6, and TNF-α by 50.7%, 47.7%, and 47.9%, respectively, compared to controls. Additionally, treatment of induced kidney stones in rats with SBCL led to a statistically significant reduction in IL-1β, IL-6, and TNF-α by 32.6%, 35.4%, and 29.7%, respectively

(Table 4). Furthermore, treatment of induced kidney stone animals with SBF resulted in a statistically significant diminution in tissue IL-1β, IL-6, and TNF-α by 24%, 28%, and 23%, respectively, compared to controls ($P \leq 0.05$) as depicted in Table 4.

Histopathological of the kidneys

The kidneys of the experimental group were evaluated using the H&E staining method (Fig. 3). Microscopically, the kidneys of the control rats, the SBCL-NEG group treated with a dose of 10 mg/kg of compound A, and the SBF-NEG group treated with a dose of 10 mg/kg of compound B, Fig. 3a–c exhibited a normal structure of the renal corpuscle, proximal tubules, and distal tubules. The renal corpuscle consisted of a glomerulus, mesangium, and Bowman's capsule, all of which were of normal size. The glomerulus consisted of a cluster of blood capillaries enclosed by a double-walled structure known as Bowman's capsule. The structure consisted of several capillary loops which were covered by endothelial cells and rested on the glomerular basement membrane. The proximal tubules consisted of significantly large cuboidal cells with brush borders and centrally placed nuclei that were rounded in shape. The structure has a slender lumen and a delicate tubular foundation membrane. The distal tubules consisted of small cuboidal cells that were weakly stained, had a large lumen, and had rounded nuclei at the top.

The experimental group, designated as the positive control, received a treatment of 5% EG. The group displayed evident pathological abnormalities, such as shrinkage of the glomerulus, enlargement of the space surrounding the renal glomerulus, substantial release of protein into the renal tubular lumen, and a frothy appearance of the tubules (Fig. 3d). The rats in the IND-EG, SBCL-EG, and SBF-EG groups (Fig. 3e–g) showed less severe pathological damage in their kidneys compared to the EG animals. However, there was some reduction in glomerular atrophy and protein exudation in the renal tubular lumen.
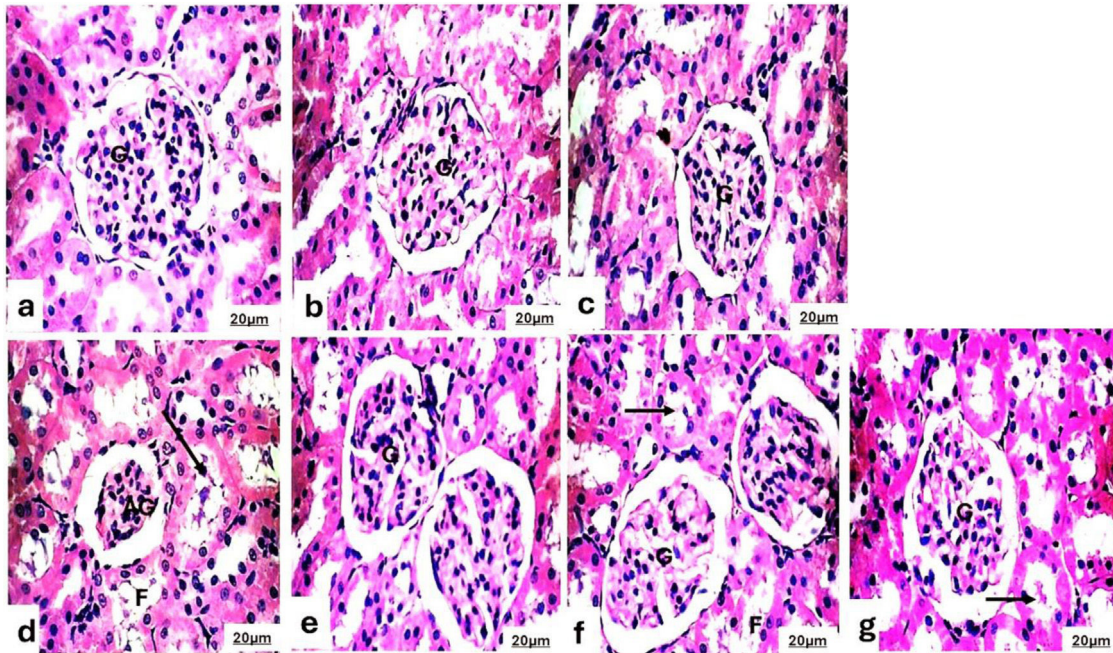
Fig. 3 – Photomicrograph of the kidneys of (a) the control rats, (b) the SBCL-NEG group treated with a dose of 10 mg/kg of compound A, and (c) the SBF-NEG group treated with a dose of 10 mg/kg of compound B exhibited a normal structure of the renal corpuscle, proximal tubules, and distal tubules. The renal corpuscle consisted of a glomerulus (G), mesangium, and Bowman's capsule, all of which were of normal size. (d) The experimental group, designated as the positive control (EG group), received a treatment of 0.12 ml of a 5% ethylene glycol solution. The group displayed evident pathological abnormalities, such as shrinkage of the glomerulus (AG), enlargement of the space surrounding the renal glomerulus, substantial release of protein into the renal tubular lumen (arrow), and a frothy appearance (F) of the tubules. The rats in the (e) IND-EG, (f) SBCL-EG, and (g) SBF-EG groups exhibited normal structure of the renal corpuscle, proximal tubules, and distal tubules. The renal corpuscle consisted of the normal glomerulus (G). However, there was some protein exudation in the renal tubular lumen (arrow) and the frothy appearance (F) of the tubules (H&E, 400×).

The transmission electron microscopy technique of the kidney

To conduct a more thorough examination of renal injury, the transmission electron microscopy technique was used to comparatively assess the ultrastructural alterations in the kidneys of both the control and experimental groups of rats. No observable damage was detected in the control group (Fig. 4a), as determined by the intactness of the basal lamina of the renal tubules in the kidney tissue.

The SBCL-NEG and the SBCL-EG groups, which received compounds A and B, respectively (Fig. 4b and c) revealed no observable harm based on the preservation of the basal lamina of renal tubules in the kidney tissue of rats. The nucleus displayed a typical morphology and was surrounded by numerous mitochondria, which varied in shape from spherical to elongated. These mitochondria exhibited abundant cristae, and the endoplasmic reticulum cisternae appeared smoothly. A few vacuoles emerged within the cytoplasm.

The experimental group, referred to as the positive control, was administered with a 5% EG (Fig. 4d). The group had clear ultrastructural abnormalities, including necrotic nuclei, degraded mitochondria, and loss of cristae in certain mitochondria, accompanied by an increase in cytoplasmic vacuoles.

The rats of the IND-EG (Fig. 4e) have a normal nucleus, but their mitochondria have deteriorated. Some of the mitochondria have lost their cristae, and there is an increase in vacuoles in the cytoplasm.

The rats in the SBCL-EG and SBF-EG groups are presented in Fig. 4f and g. The kidneys of the experimental group indicated typical ultrastructural features, similar to those of the EG group. The nucleus displayed a typical structure and was surrounded by a plentiful number of mitochondria, which varied in shape between spherical and elongated. These mitochondria were particularly rich in cristae.

Discussion

Urolithiasis, a prevalent condition with a rising global occurrence, is characterized by kidney stone formation.[48] There is widespread acknowledgment that excessive dietary salt intake correlates with an elevated risk of developing kidney stones.[49] In the present study, a high dose of EG leads to AKI, characterized by a rise in serum creatinine, urea, and BUN levels which are markers of kidney failure.

The present study showed that inducing calcium oxalate (CaOx) kidney stones using EG results in elevated serum creatinine, K^+, and PO_4^- levels. Huang et al.[50] demonstrated that hyperoxaluria in male rats, caused by 0.75% EG, can cause the
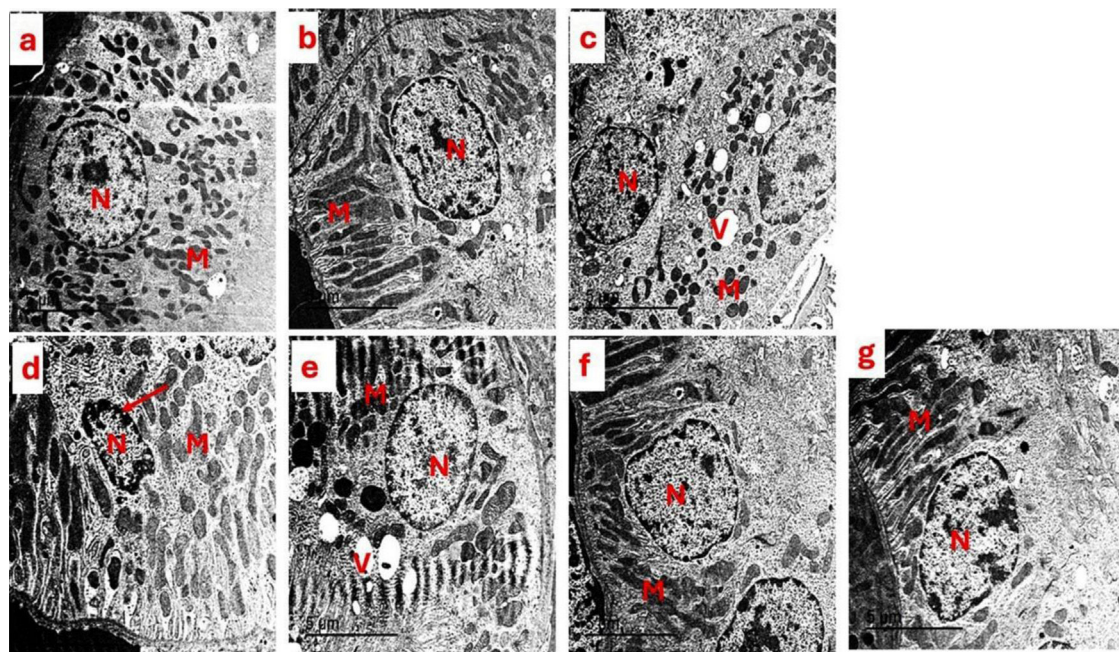
Fig. 4 – Photomicrograph of the ultrastructure of the kidney tubules of (a) control group showed normal renal tubules with normal nucleus (N) surrounded by spherical and elongated mitochondria (M). (b) The SBCL-NEG group, which received a dosage of 10 mg/kg of compound A, and (c) the SBF-NEG group, which received a dosage of 10 mg/kg of compound B exhibited no observable harm based on the preservation of the basal lamina of renal tubules in the kidney tissue of rats. The nucleus (N) displayed a typical morphology and was surrounded by numerous mitochondria (M), which varied in shape from spherical to elongated. These mitochondria exhibited abundant cristae, and the endoplasmic reticulum cisternae appeared smoothly. A few vacuoles (V) emerged within the cytoplasm. (d) The experimental positive control group (EG) that was administered 5% of EG showed clear ultrastructural abnormalities, including necrotic nucleus (N) (arrow), degraded mitochondria (M), and loss of cristae in certain mitochondria, accompanied by an increase in cytoplasmic vacuoles. (e) The IND-EG group showed a normal nucleus (N), but their mitochondria have deteriorated. Some of the mitochondria have lost their cristae, and there is an increase in vacuoles in the cytoplasm (V). (f and g) The SBCL-EG and SBF-EG groups showed a typical nucleus (N) surrounded by a plentiful number of mitochondria (M), which varied in shape between spherical and elongated. These mitochondria were particularly rich in cristae.

accumulation of CaOx crystals in the kidneys without causing metabolic acidosis. This method creates a widely accepted animal model useful for investigating the mechanisms behind human kidney stone formation.

The current study found that SBCL treatment was more beneficial for Mg^{2+} levels than indapamide standard medication in the induced kidney stones model. The variations in Mg^{2+} levels observed with these treatments indicate potential differences in their effects on magnesium regulation in the body, which could influence kidney stone formation or management.[51]

In the SBCl-NEG and SBF-NEG groups, there were no notable differences in creatinine levels compared to the control group. However, urea and uric acid levels were lower in the SBCl-NEG group than in the SBF-NEG-treated rats. Additionally, rats treated with SBF-NEG exhibited a significant increase in PTH and vitamin D levels compared to NEG and SBF-NEG-treated groups. In contrast, there were no significant changes among the SBCl-NEG, SBF-NEG, and NEG groups. Also, neither derivative compounds A nor B affected the antioxidant and inflammatory parameters of the control normal rats proving that these compounds are safe.

Creatinine levels significantly decreased in the SBF-NEG group compared to the SBCl-NEG and IND-EG groups. Additionally, urea, BUN, and uric acid levels were higher in the SBF-NEG group than in the SBCl-NEG group. However, in IND-EG treatment urea and BUN levels increased more than treatment with both derivatives in induced kidney stone rats. Furthermore, IND-EG demonstrated a reduction in oxidative stress and inflammatory biomarkers alongside an increase in antioxidants when compared to treatment with compounds A and B. However, SBCl-NEG exhibited superior effects on antioxidant and inflammatory parameters than SBF-NEG.

The findings of this study revealed an elevation in PTH and CT levels following kidney stone induction, accompanied by a reduction in vitamin D levels. Vitamin D deficiency promotes inflammation and oxidative stress.[52] Therefore, it is important to note that vitamin D deficiency can worsen the formation or severity of kidney stones. Studies suggest that vitamin D inhibits the production of pro-inflammatory cytokines and activating its receptor (VDR) has been demonstrated to suppress nuclear factor-kappa B (NF-κB) activation. *In vitro* and animal model studies have confirmed that VDR activation by vitamin D inhibits renin gene transcription, potentially damp-

ening oxidative stress. There seems to be a high prevalence of vitamin D deficiency among individuals susceptible to developing kidney stones.[53]

Ruiz-Sánchez et al.[54] observed that primary hyperparathyroidism (PHPT) is a prevalent endocrine disorder marked by elevated levels of calcium (hypercalcemia) and high or inappropriately normal levels of PTH as shown in the present study. Renal complications are a significant concern in PHPT, with silent nephrolithiasis. A confirmed relationship exists between urinary calcium levels and affected individuals' risk of kidney stones.

In this study, the EG group exhibited elevated levels of LPO, NO, and PC, along with decreased levels of GSH and activity of SOD, indicating an imbalance in oxidative/antioxidant mechanisms. This imbalance suggests that oxidative stress could lead to tubular damage, resulting in crystal retention in renal tubules and subsequent stone formation, as proposed by Tavasoli and Taheri.[55] These findings, supported by Khan and Canales,[56] suggest that deficiencies in antioxidants are common among individuals prone to developing kidney stones and may contribute to stone formation by causing oxidative damage to cells.

In the current investigation, a high concentration of ROS in induced kidney stone rats accelerates the progression of an inflammatory response. Krishnan et al.[57] found that the significance of inflammation is underscored by the strong association between renal tubular epithelial cells and crystals. This interaction is pivotal, facilitating the generation of pro-inflammatory proteins like TNF-α and IL-1β through macrophage activation. Excessive ROS production may act simultaneously as both a catalyst and a result of inflammation, forming a vicious cycle wherein tubular damage from crystal presence triggers inflammation that fosters crystal formation.[58]

In the current study, we investigated the antiurolithiatic activity of compound A (SBCL) and compound B (SBF) and compared it with the activity of the indapamide standard drug. The animals were treated with compound A (SBCL), compound B (SBF), and indapamide to dissolve the stones induced by the administration of EG. Compounds A and B showed significant improvement changes in all the measured parameters compared to the EG group.

Uric acid, BUN, urea, and creatinine levels are the most reliable biochemical indicators utilized to evaluate the extent of renal tissue damage. Consequently, in cases of cellular injury, there is a buildup of these substances in the bloodstream.[59] Uric acid, BUN, urea, and creatinine levels were reduced by treatment with compounds A and B to levels similar to indapamide.

Oxalate levels in urine and serum are critical indicators of kidney health, particularly in the context of kidney stone formation.[60] Elevated oxalate concentrations can contribute to the development of calcium oxalate stones, the most common type of kidney stones.[61] Therefore, managing oxalate levels in both serum and urine is essential for preventing and treating kidney stones.[62] Treatments such as SBCL, SBF, and indapamide show promise in reducing oxalate concentrations, thereby mitigating the risk of stone formation and promoting kidney health.

Thus, pharmacological preparations of compounds A and B may be beneficial for treating nephrolithiasis and the disorders related to oxidation. Urea, creatinine, and uric acid levels accumulate in the blood. Also, increased lipid peroxidation and decreased levels of antioxidant potential have been reported in the kidneys of rats treated with EG.

The effect of benzene sulfonamide derivatives on antioxidant and inflammatory responses in induced kidney stone conditions involves several key mechanisms. These derivatives have been found to modulate nitrogenous waste in the blood, and oxidative stress levels by enhancing the activity of antioxidant enzymes, such as SOD and CAT, thereby reducing the accumulation of ROS in the kidney tissue.[63] Additionally, they exhibit anti-inflammatory properties by decreasing the production of pro-inflammatory cytokines and mediators, such as interleukin-1β and TNF-α, which are known to exacerbate kidney stone formation and associated tissue damage.[64]

Moreover, benzene sulfonamide derivatives have been shown to suppress the activation of NF-κB, a transcription factor intricate in regulating inflammatory responses, thus mitigating the inflammatory cascade triggered by kidney stone induction.[65] By targeting both oxidative stress and inflammation pathways, these derivatives can save kidney function and reduce tissue injury associated with kidney stone formation.[66]

Furthermore, studies have indicated that benzene sulfonamide derivatives may also exert direct effects on the crystallization process, inhibiting the formation and growth of kidney stones by interfering with the aggregation of stone-forming crystals, such as CaOx or calcium phosphate.[67] Overall, the impact of benzene sulfonamide derivatives on antioxidant and inflammatory responses in induced kidney stone conditions highlights their potential therapeutic benefits in mitigating the progression of kidney stone disease and associated complications.

Histopathological and ultrastructure exposed non-significant findings in the control rats. However, the positive group displayed glomerular atrophy and protein cast in the lumen of the tubules. In the indapamide drug, compound A and compound B treatment groups, there was a reduction in glomerular atrophy and protein cast in the lumen of the tubules was apparent. This can occur because EG produces toxic metabolic waste products known as ROS. Issac et al.[68] explained that ROS compounds interact with cellular molecules, leading to damage in the glomerulus. This damage impairs the function of the filtration organ, resulting in glomerular atrophy.

Histopathology indicated acute alterations in kidney tissues, including tubular dilation, deposition, and damage of red blood cells in the glomeruli, interstitial inflammation, and the presence of oxalate crystals. However, there were no clear marks of chronic kidney damage such as glomerular hurt or deterioration, stark tubular obliteration, or wide fibrosis. Hence, characterizing the condition as AKI remains suitable for the study period.

Treatment of the EG group with indapamide drug, compound A, and compound B has been able to restore the size of the glomerulus. The expansion of Bowman's capsule space occurs due to glomerular atrophy, which is a reduction in

tissue size caused by necrosis, poor circulation, or oxygen deprivation.[69]

Electron microscopic examination of kidney sections of the EG group revealed ultrastructural alteration in proximal and distal tubules when compared to the control group. The mitochondria of the kidney sections of the EG group are cristolysis. Similar mitochondrial degeneration of their crista c has been demonstrated in kidney tubular cells subjected to stress.[70] These findings are in parallel with Giermaziak and Orkisz,[71] who demonstrated that EG intoxication destroys cytoplasmic organelles, particularly mitochondria. Moreover, McMartin and Wallace[72] found that EG-induced proximal tubular necrosis leads to loss of renal role. Treatment of the EG group with indapamide drug, compounds A, and B showed variable degrees of improvement of proximal and distal tubules.

Conclusion

In conclusion, the study demonstrated that induction of kidney stones by EG increased kidney function tests, PTH, calcitonin, oxidative, inflammatory marks, and decreased vitamin D levels and antioxidants. The influence of benzene sulfonamide derivatives on antioxidant and inflammatory reactions under induced kidney stone conditions underscores their potential therapeutic advantages in alleviating the advancement of kidney stone disease and its related complications. Moreover, it improved EG-induced histopathological alterations and reduced crystal deposition in kidney tissue. Both compounds were discovered to have equal potency in preventing the stone's formation. However, SBCl-EG exhibited superior effects on antioxidant and inflammatory parameters than SBF-EG. Although the mechanism of action remains unclear, their antioxidant properties and anti-inflammatory content may contribute to their efficacy. Additional research is necessary to elucidate their mechanism of action further.

Ethical approval and consent to participate

This animal experiment was performed following EU Directive 2010/63/EU and compliance with ARRIVE guidelines, which were strictly followed to minimize the suffering of the animal during the experiments. The experimental work was approved by the Institutional Animal Ethics Committee of the Faculty of Science Animal Ethics Committee, Suez Canal University, with number: REC166/2022.

Funding

Authors' contributions

A.E., Z.N., H.N., M.N., and N.S. wrote the main manuscript text, and A.E. and H.N. prepared Figs. 2 and 3. All authors reviewed the manuscript.

Consent for publication

Not applicable.

Competing interests

The authors declare no competing interest.

Acknowledgments

REFERENCES

1. Wang Z, Zhang Y, Zhang J, Deng Q, Liang H. Recent advances in the mechanisms of kidney stone formation. Int J Mol Med. 2021;48:1–10.
2. Devi AT, Nagaraj R, Prasad A, Lakkappa DB, Zameer F, Nagalingaswamy NPM. Nephrolithiasis: insights into biomimics, pathogenesis, and pharmacology. Clin Complement Med Pharmacol. 2023;3:100077.
3. Tzou DT, Taguchi K, Chi T, Stoller ML. Animal models of urinary stone disease. Int J Surg. 2016;36:596–606.
4. Alford A, Furrow E, Borofsky M, Lulich JJNRU. Animal models of naturally occurring stone disease. Nat Rev Urol. 2020;17:691–705.
5. Dahl NK, Goldfarb DS. Nutritional prevention and treatment of urinary tract stones. In: Nutritional management of renal disease. Elsevier; 2022. p. 685–97.
6. Tamborino F, Cicchetti R, Mascitti M, Litterio G, Orsini A, Ferretti S, et al. Pathophysiology and main molecular mechanisms of urinary stone formation and recurrence. Int J Mol Sci. 2024;25:3075.
7. Vinciya T. Evaluation of antiurolithiatic activity of ethanolic and aqueous extract of phaseolus vulgaris linn seeds. Madurai: Ultra College of Pharmacy; 2018.
8. Stamatelou K, Goldfarb DS. Epidemiology of kidney stones. Healthcare. 2023;11:424.
9. Bollner MR, MPAS P. Kidney stones. Urology. 2017;3:37.
10. Akram M, Jahrreiss V, Skolarikos A, Geraghty R, Tzelves L, Emilliani E, et al. Urological guidelines for kidney stones: overview and comprehensive update. J Clin Med. 2024;13:1114, http://dx.doi.org/10.3390/jcm13041114.
11. Challacombe B, Bultitude MF. The kidneys, urinary tract, and prostate. In: Browse's introduction to the symptoms & signs of surgical disease. CRC Press; 2021. p. 573–87.
12. Stojanović NM, Mitić KV, Nešić M, Stanković M, Petrović V, Baralić M, et al. Oregano (*Origanum vulgare*) essential oil and its constituents prevent rat kidney tissue injury and inflammation induced by a high dose of L-arginine. Int J Mol Sci. 2024;25:941.
13. Sharifi-Rad M, Anil Kumar NV, Zucca P, Varoni EM, Dini L, Panzarini E, et al. Lifestyle, oxidative stress, and antioxidants: back and forth in the pathophysiology of chronic diseases. Front Physiol. 2020;11:694.
14. Chen X, Shi C, Wang Y, Yu H, Zhang Y, Zhang J, et al. The mechanisms of glycolipid metabolism disorder on vascular injury in type 2 diabetes. Front Physiol. 2022;13:952445.

15. Xing J, Cai H, Lin Z, Zhao L, Xu H, Song Y, et al. Examining the function of macrophage oxidative stress response and immune system in glioblastoma multiforme through analysis of single-cell transcriptomics. Front Immunol. 2024;14:1288137.

16. Srivastava A, Tomar B, Sharma D, Rath SK. Mitochondrial dysfunction and oxidative stress: role in chronic kidney disease. Life Sci. 2023;319:121432.

17. Choudhury D, Ahmed Z. Drug-associated renal dysfunction and injury. Nat Clin Pract Nephrol. 2006;2:80–91.

18. Derakhshandeh-Rishehri S-M, Franco LP, Hua Y, Herder C, Kalhoff H, Frassetto LA, et al. Higher renal net acid excretion, but not higher phosphate excretion, during childhood and adolescence associates with the circulating renal tubular injury marker interleukin-18 in adulthood. Int J Mol Sci. 2024;25:1408.

19. Blantz RC, Munger KJN. Role of nitric oxide in inflammatory conditions. Nephron. 2002;90:373–8.

20. Peng K, Zheng Y, Xia W, Mao Z-W. Organometallic anti-tumor agents: targeting from biomolecules to dynamic bioprocesses. Chem Soc Rev. 2023;52:2790–832.

21. Ernst ME, Fravel MA. Thiazide and the thiazide-like diuretics: review of hydrochlorothiazide, chlorthalidone, and indapamide. Am J Hypertens. 2022;35:573–86.

22. Dzau V. The cardiovascular continuum and renin–angiotensin–aldosterone system blockade. J Hypertens. 2005;23:S9–17.

23. Supuran CT. Drug interactions of carbonic anhydrase inhibitors and activators. Eur J Med Chem. 2024;20:143–55.

24. Germino F. The management and treatment of hypertension. Clin Cornerstone. 2009;9:S27–33.

25. Chan TY. Indapamide-induced severe hyponatremia and hypokalemia. Ann Pharmacother. 1995;29:1124–8, http://dx.doi.org/10.1177/106002809502901111.

26. Alani BG, Salim KS, Mahdi AS, Al-Temimi AA. Sulfonamide derivatives: synthesis and applications. Int J Front Chem Pharm Res. 2024;4, http://dx.doi.org/10.53294/ijfcpr.2024.4.1.0021, 001–015.

27. Fallahzadeh MA, Dormanesh B, Fallahzadeh MK, Roozbeh J, Fallahzadeh MH, Sagheb MM. Acetazolamide and hydrochlorothiazide followed by furosemide versus furosemide and hydrochlorothiazide followed by furosemide for the treatment of adults with nephrotic edema: a randomized trial. Am J Kidney Dis. 2017;69:420–7.

28. Ragab MA, Eldehna WM, Nocentini A, Bonardi A, Okda HE, Elgendy B, et al. 4-(5-Amino-pyrazol-1-yl) benzenesulfonamide derivatives as novel multi-target anti-inflammatory agents endowed with inhibitory activity against COX-2, 5-LOX and carbonic anhydrase: design, synthesis, and biological assessments. Eur J Med Chem. 2023;250:115180.

29. Albujuq NR, Althumayri K, Alharbi RAK, Al-Karmalawy AA, Nafie MS. Design and synthesis of benzenesulfonamides coupled with piperidine, morpholine, and N,N-dimethylethanamine moieties as apoptotic inducers through VEGFR2 and topoisomerase II inhibition. ChemistrySelect. 2023;8:e202301315, http://dx.doi.org/10.1002/slct.202301315.

30. Guillén J, Prins J-B, Howard B, Degryse A-D, Gyger M. Chapter 5 – The European Framework on Research Animal Welfare Regulations and Guidelines. In: Guillén J, editor. Laboratory animals. second edition Academic Press; 2018. p. 117–202.

31. Zhai W, Zheng J, Yao X, Peng B, Liu M, Huang J, et al. Catechin prevents the calcium oxalate monohydrate-induced renal calcium crystallization in NRK-52E cells and the ethylene glycol-induced renal stone formation in rat. BMC Complement Altern Med. 2013;13:1–11, http://dx.doi.org/10.1186/1472-6882-13-228.

32. Sumitra M, Manikandan P, Rao KVK, Nayeem M, Manohar BM, Puvanakrishnan R. Cardiorespiratory effects of diazepam–ketamine, xylazine–ketamine, and thiopentone anesthesia in male Wistar rats – a comparative analysis. Life Sci. 2004;75:1887–96.

33. Jo EJ, Bae E, Yoon J-H, Kim JY, Han JS. Comparison of murine retroorbital plexus and facial vein blood collection to mitigate animal ethics issues. Lab Anim Res. 2021;37:12, http://dx.doi.org/10.1186/s42826-021-00090-4.

34. Vázquez M, Mikhelson K, Piepponen S, Rämö J, Sillanpää M, Ivaska A, et al. Determination of Na$^+$, K$^+$, Ca^{2+}, and Cl$^-$ ions in wood pulp suspension using ion-selective electrodes. Electroanalysis. 2001;13:1119–24, http://dx.doi.org/10.1002/1521-4109(200109)13:13.

35. Mohabbati-Kalejahi E, Azimirad V, Bahrami M, Ganbari A. A review on creatinine measurement techniques. Talanta. 2012;97:1–8, http://dx.doi.org/10.1016/j.talanta.2012.04.005.

36. Fujita T, Takata S, Sunahara Y. Enzymatic rate assay of creatinine in serum and urine. Clin Chem. 1993;39:2130–6, http://dx.doi.org/10.1093/clinchem/39.10.2130.

37. Yasmin F, Samad N. Association between serum electrolytes and erythrocytes Na$^+$, K$^+$ in hypertensive and normotensive male compared to female. Pak J Pharm Sci. 2020;33:207–14.

38. Karamad D, Khosravi-Darani K, Hosseini H, Tavasoli S, Miller AW. Evaluation of *Oxalobacter formigenes* DSM 4420 biodegradation activity for high oxalate media content: an in vitro model. Biocatal Agric Biotechnol. 2019;22:101378.

39. Wu L, Zhang G, Lu Q, Sun Q, Wang M, Li N, et al. Evaluation of salmon calcitonin (sCT) enteric-coated capsule for enhanced absorption and GI tolerability in rats. Drug Dev Ind Pharm. 2010;36:362–70, http://dx.doi.org/10.3109/03639040903173580.

40. AlQuaiz AM, Mujammami M, Kazi A, Hasanato RM, Alodhayani A, Shaik SA, et al. Vitamin D cutoff point in relation to parathyroid hormone: a population based study in Riyadh city, Saudi Arabia. Arch Osteoporos. 2019;14:22, http://dx.doi.org/10.1007/s11657-019-0565-6.

41. Carracedo J, Ramírez-Carracedo R, Martínez de Toda I, Vida C, Alique M, De la Fuente M, et al. Protein carbamylation: a marker reflecting increased age-related cell oxidation. Int J Mol Sci. 2018;19:1495.

42. Paoletti F, Mocali A. Determination of superoxide dismutase activity by purely chemical system based on NAD(P)H oxidation. In: Methods in enzymology. Academic Press; 1990. p. 209–20.

43. Kim C-Y, Lee C, Park GH, Jang J-H. Neuroprotective effect of epigallocatechin-3-gallate against β-amyloid-induced oxidative and nitrosative cell death via augmentation of antioxidant defense capacity. Arch Pharm Res. 2009;32:869–81, http://dx.doi.org/10.1007/s12272-009-1609-z.

44. Dalle-Donne I, Rossi R, Giustarini D, Milzani A, Colombo R. Protein carbonyl groups as biomarkers of oxidative stress. Clin Chim Acta. 2003;329:23–38, http://dx.doi.org/10.1016/S0009-8981(03)00003-2.

45. Çetin A, Sen A, Çetin I, Çimen B, Cimen L, Savas G, et al. Comparison of ELISA and flow cytometry for measurement of interleukin-1 beta, interleukin-6, and tumor necrosis factor-α. Turkish J Biochem. 2018;43:540–8, http://dx.doi.org/10.1515/tjb-2017-0164.

46. Alturkistani HA, Tashkandi FM, Mohammedsaleh ZM. Histological stains: a literature review and case study. Glob J Health Sci. 2015;8:72–9, http://dx.doi.org/10.5539/gjhs.v8n3p72.

47. El Hak HNG, Metawea SI, Nabil ZI. Fenugreek (*Trigonella foenum graecum* L.) supplementation safeguards male mice from aflatoxin B1-induced liver and kidney damage. Comp Clin Pathol. 2022;31:925–42, http://dx.doi.org/10.1007/s00580-022-03413-6.

48. O'Kell AL, Grant DC, Khan SR. Pathogenesis of calcium oxalate urinary stone disease: species comparison of humans, dogs, and cats. Urolithiasis. 2017;45:329–36.

49. Zeng H, Liu Z, He Y, Chen H, He J, Liu M, et al. Multivitamins co-intake can reduce the prevalence of kidney stones: a large-scale cross-sectional study. Int Urol Nephrol. 2024;2024:1–11, http://dx.doi.org/10.1007/s11255-024-04021-9.

50. Huang H-S, Ma M-C, Chen J. Low-vitamin E diet exacerbates calcium oxalate crystal formation via enhanced oxidative stress in rat hyperoxaluric kidney. Am J Physiol Renal Physiol. 2009;296:F34–45, http://dx.doi.org/10.1152/ajprenal.90309.2008.

51. Musso CG. Magnesium metabolism in health and disease. Int Urol Nephrol. 2009;41:357–62, http://dx.doi.org/10.1007/s11255-009-9548-7.

52. Wimalawansa SJ. Vitamin D deficiency: effects on oxidative stress, epigenetics, gene regulation, and aging. Biology. 2019;8:30.

53. Letavernier E, Daudon M. Vitamin D, hypercalciuria and kidney stones. Nutrients. 2018;10:366.

54. Ruiz-Sánchez JG, Pazos Guerra M, Meneses D, Runkle I. Primary hyperaldosteronism: when to suspect it and how to confirm its diagnosis. Endocrines. 2022;3:29–42.

55. Tavasoli S, Taheri M. Vitamin D and calcium kidney stones: a review and a proposal. Int Urol Nephrol. 2019;51:101–11, http://dx.doi.org/10.1007/s11255-018-1965-z.

56. Khan SR, Canales BK. Proposal for pathogenesis-based treatment options to reduce calcium oxalate stone recurrence. Asian J Urol. 2023;10:246–57, http://dx.doi.org/10.1016/j.ajur.2023.01.008.

57. Krishnan N, Moledina DG, Perazella MA. Toxic nephropathies of the tubulointerstitium: core curriculum 2024. Am J Kidney Dis. 2024;83:659–76, http://dx.doi.org/10.1053/j.ajkd.2023.09.017.

58. Xiong P, Zheng Y-Y, Ouyang J-M. Carboxylated Pocoa polysaccharides inhibited oxidative damage and inflammation of HK-2 cells induced by calcium oxalate nanoparticles. Biomed Pharmacother. 2023;169:115865, http://dx.doi.org/10.1016/j.biopha.2023.115865.

59. Lisowska-Myjak B. Serum and urinary biomarkers of acute kidney injury. Blood Purif. 2010;29:357–65.

60. Mitchell T, Kumar P, Reddy T, Wood KD, Knight J, Assimos DG, et al. Dietary oxalate and kidney stone formation. Am J Physiol Renal Physiol. 2019;316:F409–13.

61. Massey LK, Roman-Smith H, Sutton RA. Effect of dietary oxalate and calcium on urinary oxalate and risk of formation of calcium oxalate kidney stones. J Am Diet Assoc. 1993;93:901–6.

62. Frassetto L, Kohlstadt I. Treatment and prevention of kidney stones: an update. Am Fam Physician. 2011;84:1234–42.

63. Abdel-Rahman Mohamed A, Khater SI, Metwally MMM, Bin Emran T, Nassan MA, Abd El-Emam MM, et al. TGF-β1, NAG-1, and antioxidant enzymes expression alterations in cisplatin-induced nephrotoxicity in a rat model: comparative modulating role of melatonin, Vit. E and ozone. Gene. 2022;820:146293, http://dx.doi.org/10.1016/j.gene.2022.146293.

64. Wigner P, Grebowski R, Bijak M, Szemraj J, Saluk-Bijak J. The molecular aspect of nephrolithiasis development. Cells. 2021;10:1926.

65. Liu Z, Deng P, Liu S, Bian Y, Xu Y, Zhang Q, et al. Is nuclear factor erythroid 2-related factor 2 a target for the intervention of cytokine storms? Antioxidants. 2023;12:172.

66. Zhang Y-H, Xian J-Y, Li S-J, Li C-Y, Yu B-X, Liang Q, et al. Hydroxycitric acid inhibits kidney stone through crystallization regulation and reduction of hyperoxalate-induced lipotoxicity. J Funct Foods. 2023;105:105561, http://dx.doi.org/10.1016/j.jff.2023.105561.

67. Tienda-Vázquez MA, Morreeuw ZP, Sosa-Hernández JE, Cardador-Martínez A, Sabath E, Melchor-Martínez EM, et al. Nephroprotective plants: a review on the use in pre-renal and post-renal diseases. Plants. 2022;11:818, http://dx.doi.org/10.3390/plants11060818.

68. Issac PK, Velayutham M, Guru A, Sudhakaran G, Pachaiappan R, Arockiaraj J. Protective effect of morin by targeting mitochondrial reactive oxygen species induced by hydrogen peroxide demonstrated at a molecular level in MDCK epithelial cells. Mol Biol Rep. 2022;49:4269–79, http://dx.doi.org/10.1007/s11033-022-07261-z.

69. Forbes MS, Thornhill BA, Chevalier RL. Proximal tubular injury and rapid formation of tubular glomeruli in mice with unilateral ureteral obstruction: a new look at an old model. Am J Physiol Renal Physiol. 2011;301:F110–7.

70. Xu Y, Ruan S, Wu X, Chen H, Zheng K, Fu B. Autophagy and apoptosis in tubular cells following unilateral ureteral obstruction are associated with mitochondrial oxidative stress. Int J Mol Med. 2013;31:628–36.

71. Giermaziak H, Orkisz S. Effects of ethylene glycol on the ultrastructure of hepatocytes. Exp Toxicol Pathol. 1995;47:359–65, http://dx.doi.org/10.1016/S0940-2993(11)80348-9.

72. McMartin KE, Wallace KB. Calcium oxalate monohydrate, a metabolite of ethylene glycol, is toxic for rat renal mitochondrial function. Toxicol Sci. 2004;84:195–200, http://dx.doi.org/10.1093/toxsci/kfi062.